Green Chemistry

Accepted Manuscript

ROYAL SOCIETY OF CHEMISTRY

www.rsc.org/greenchem

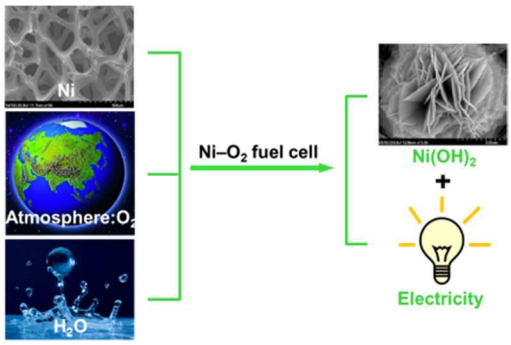

A totally atom-economical route to synthesize nickel hydroxide with a desired nano/micro structure is realized by using a membrane-free Ni–O_2 fuel cell.

Atom-Economical Synthesis of Nano/Micro Structured Nickel Hydroxide Realized by an Ni–O_2 Fuel Cell

Junqing Pan[1,4]*, Meng Yang[1], Yanzhi Sun[2,4], Ting Ma[1], Xihong Yue[1], Wei Li[3]*, Xueliang Sun[4]

[1]State Key Laboratory of Chemical Resource Engineering, Beijing University of Chemical Technology, Beijing 100029, China

[2]National Fundamental Research Laboratory of New Hazardous Chemicals Assessment and Accident Analysis, Beijing University of Chemical Technology, Beijing 100029, China

[3]Department of Engineering Technology and Texas Center for Superconductivity, University of Houston, Houston, TX 77204, USA

[4]Department of Mechanical and Materials Engineering, University of Western Ontario, London, ON, N6A 5B9, Canada.

*Correspondence to: jqpan@mail.buct.edu.cn; wli23@central.uh.edu

Abstract

The conventional syntheses of nickel hydroxide ($Ni(OH)_2$) produce a large amount of chemical wastes because of low atom-economy reactions employed in the processes. Here, we describe an atom-economical synthesis of $Ni(OH)_2$ from nickel metal, water, and oxygen gas (O_2) through a newly designed, membrane-free nickel–oxygen (Ni–O_2) fuel cell. Electricity is also generated as the by-product. The new synthesis method can greatly reduce the pollution to the environment. The as-prepared $Ni(OH)_2$ has a desired nano/micro structure and exhibits excellent performance as the positive electrode material of nickel-metal hydride batteries.

Introduction

Lately, a tremendous of research has been conducted on the development of new electrode materials for advanced batteries, such as nickel–metal hydride (Ni/MH) and lithium-ion batteries, as the power sources for electric vehicles to reduce the pollution from transportation. However, less attention has been paid to the environmental pollution and energy consumption caused by the synthesizing processes of the electrode materials.[1-5] The widespread usage of the environmentally benign electric vehicles requires the development of green approaches with high atom economy to synthesize the materials. These approaches have a high proportion of reactant atoms incorporated into the desired product.

Nickel hydroxide ($Ni(OH)_2$) is the active material for the positive electrodes of NiMH batteries[6-8] and also an important precursor of the positive electrode materials for lithium ion batteries.[9-11] It is typically synthesized from the reactions of a nickel salt, *e.g.*, nickel sulfate ($NiSO_4$), and an alkali, *e.g.*, sodium hydroxide (NaOH).[12-19] The high purity $NiSO_4$ is usually synthesized by dissolving metallic nickel (Ni) in a sulfuric acid solution containing nitric acid or hydrogen peroxide as the oxidant in industrial processes.[20] The flowchart of a common existing process for the preparation of $Ni(OH)_2$ is shown in Schematic 1a. This process is atom-uneconomical because a large quantity of unwanted acids and salt are generated from the reaction A1 and reaction A2.[21, 22] The atom economy of this route is 21.6%, as the calculation shown in the supplementary information.

Atom economy is defined as a measure of the proportion of reactant atoms which are incorporated into the desired product of a chemical reaction.[21] From the view of atom economy, the best route to synthesize $Ni(OH)_2$ is the direct reaction of metallic Ni, oxygen gas (O_2), and water (H_2O), in which all of the reactants are converted into the product to get an 100% of atom

economy (Schematic 1b). This reaction is thermodynamically allowed at room temperature with a release of 216.3 kJ mol^{-1} Gibbs free energy. However, it is not kinetically favorable because of two main reasons. One reason is that the Ni metal surface is invariably passivated by a dense nickel oxide film as a barrier for reaction, known as deactivation. The oxide film is formed instantly when the metallic nickel is exposed to air and/or water,[23] or even formed when it is in highly corrosive hydrofluoric acid (HF).[24] The other reason is that the O_2 gas has a very low solubility in water, resulting in a very low concentration in the system for reaction. Besides, as the active material for the electrodes in batteries, the synthesized $Ni(OH)_2$ needs to have a certain ordered crystalline structure to obtain excellent electrochemical activities.

Herein, we describe an 100% atom-economical synthesis of $Ni(OH)_2$ from Ni metal, water and O_2 based on a newly designed Ni–O_2 fuel cell, which consists of an Ni foam anode, an oxygen cathode electrode with Pt/C catalyst on the carbon paper, and an aqueous electrolyte. The key to realize this route is the activation of the Ni anode. $Ni(OH)_2$ has been synthesized at a high rate after addressing this challenge and the samples exhibited excellent performances in NiMH batteries.

Results and discussion

Fig. 1 illustrates the schematic of the Ni–O_2 fuel cell, designed to synthesize the nano/micro-structured $Ni(OH)_2$. The fuel cell consists of an Ni foam anode, an oxygen cathode, and an aqueous electrolyte. The optimized electrolyte has a pH in the range of 11.30–11.50 (adjusted by NaOH), and comprises of 0.50 mol L^{-1} sodium sulfate (Na_2SO_4, 99.5%,), 0.60 mol L^{-1} sodium chloride (NaCl, 99.5%), and 2.0 mol L^{-1} aqua ammonia ($NH_3 \cdot H_2O$, 25%). The Na_2SO_4 and NaCl were, respectively, used as the supporting electrolyte and activating agent for the Ni anodic

dissolution. The $NH_3 \cdot H_2O$ was used as the complexation agent. The selection and optimization of this composition will be thoroughly discussed hereunder.

The $Ni(OH)_2$ is synthesized by electrochemical reactions and complexation–precipitation reaction as shown in Eq. 1–4. In the cell, the Ni foam anode undergoes electro-oxidation reaction, or anodic dissolution, to produce $Ni(NH_3)_6^{2+}$ and releases electrons (Eq. 1). The electrons travel through the external electric circuit, do electric work, and arrive at the cathode. O_2 is fed into the cathode, where it is electro-chemically reduced with water and the electrons from the anode to produce OH^- ions (Eq. 2). Though the anode and cathode compartments are separated to protect the freshly produced $Ni(NH_3)_6^{2+}$ and OH^- ions from the instant combination, the internal circuit is formed by the transport of $Ni(NH_3)_6^{2+}$ and OH^- ions through the pipe joints before and after the compartments. The two electro-chemical reactions of Eq. 1 and 2 and the chemical reaction of Eq. 3 combine into the overall reaction of the fuel cell (Eq. 4). The positive standard potential of 0.881 V means that the reaction of metallic Ni, O_2, and water to synthesize $Ni(OH)_2$ can spontaneously occur in the Ni–O_2 fuel cell.

Eq. 1 : $Ni + 6NH_3 \cdot H_2O - 2e^- = Ni(NH_3)_6^{2+} + 6H_2O$ (anodic reaction, $E° = -0.480$ V)

Eq. 2 : $1/2O_2 + H_2O + 2e^- = 2OH^-$ (cathodic reaction, $E° = 0.401$V)

Eq. 3 : $Ni(NH_3)_6^{2+} + 2OH^- = Ni(OH)_2 + 6NH_3$ (complexation–precipiation reaction)

Eq. 4 : $Ni + 1/2O_2 + H_2O = Ni(OH)_2$ (overal reaction of the fuel cell, $E° = 0.401 - (-0.480) = 0.881$ V)

As the reactions of Eq. 1 and 2 continue, the concentrations of $Ni(NH_3)_6^{2+}$ and OH^- ions increase to the saturation points for the appearance of the nuclei of $Ni(OH)_2$. They move along with the flow of electrolyte in the pipe system and enter the electrolyte tank, where the $Ni(OH)_2$ nuclei undergo crystal nucleation and growth to micro powders.[19] It needs to be mentioned that

both pipe system and the tank are heated to the fuel cell temperature to avoid the precipitation of $Ni(OH)_2$ by a lower temperature. The small particles can dissolve through complexation dissolution process and then re-precipitate on the surface of the large $Ni(OH)_2$ particles. This precipitation-complexation dissolution is a dynamic process, which helps to generate spherical $Ni(OH)_2$ powders with the desired nano/micro structure/morphology for NiMH batteries.[19]

The formed $Ni(OH)_2$ powders reside in the tank by the block of a frit filter. The filtrate is pumped back into the fuel cell for the consecutive reactions, when the concentrations of $(NH_3)_6^{2+}$ and OH^- are at the saturation point. These concentrations increase again through the reactions in the cell and $Ni(OH)_2$ nuclei are kept produced by the reaction of Eq. 3 in the exist pipe system and collected in the tank to form $Ni(OH)_2$ powders.

Activation of the electrodes needs to be investigated to improve the performance of the Ni–O_2 fuel cell and thus to produce more $Ni(OH)_2$. The oxygen cathode has been extensively investigated as it is a common cathode for low temperature fuel cells, such as proton exchange membrane fuel cells, direct methanol fuel cells, etc. The Ni anode, on the contrary, has not been reported as the anode for a fuel cell and thus it is investigated herein for the newly proposed Ni–O_2 fuel cell. Ni metal is known to be easily passivated by forming oxides in the environment.[23] When it is used as an anode, the passivation becomes more severe owing to more oxides produced by oxidation reactions, leading to a significant increase of the polarization of its anodic dissolution. To make the new route feasible to synthesize $Ni(OH)_2$, the Ni anode needs to be prevented from the passivation and kept activated during the anodic dissolution process. Here we demonstrate the investigation with an Ni foam anode rather an Ni plate anode because Ni foam anode produced a larger current with a larger surface area, as shown in Fig. S1. Study on activation with an Ni plate anode will be conducted in the future.

The effect of $NH_3 \cdot H_2O$ concentration on the anodic polarization is shown in Fig. 2a. As the concentration increases, the anodic reaction (Eq. 2) moves forward, resulting in the increase of the anodic current. It also suppresses the combination of $Ni(NH_3)_6^{2+}$ and OH^- to produce $Ni(OH)_2$ (Eq. 3) on the surface, by which the anode surface passivation by the $Ni(OH)_2$ is mitigated. The anodic current density reaches the maximum value of 9.0 mA cm^{-2}, equivalent to an $Ni(OH)_2$ production rate of 15.6 mg h^{-1} cm^{-2}, at 2.0 mol L^{-1} concentration of $NH_3 \cdot H_2O$ and hardly further increases with the concentration.

It is known that halogen ions can destruct metal oxide films and an applicable example was demonstrated by activating aluminum, an active metal similar to Ni, as an effective reducing agent for wet-chemical synthesis through the addition of halogen ions.[25] Further activation of the Ni anode was conducted in this study by comparing the effects of different halogen ions. As shown in Fig. 2b, the anodic current densities with the existence of halogen ions are much larger than the current density without halogen ions. The FE-SEM images of the Ni anode before and after anodic dissolution in Fig. 2c and 2d show the evidence of the surface corrosion. Moreover, the anodic current densities decrease in the order of $Cl^- > Br^- > I^-$, which can be explained that a smaller ion is easier to penetrate the oxide film.[25] The anodic polarization with F^- ions is exceptional to this trend owing to three reasons: the F^- ions keep hydration when attacking the passive oxide film, the formed NiF_2 contributes to the passivation film on the Ni surface, and NiF_2 has a lower solubility than $NiCl_2$.[23, 26-28]

The Cl^- concentration was then optimized for the anodic dissolution of the Ni anode. Fig. 2e shows that the anodic current substantially increases as the Cl^- concentration increases from 0.10 to 0.60 mol L^{-1}. Further increase of the concentration does not significantly increase the current,

suggesting that the activation process with 0.60 mol L^{-1} of Cl^- is fast enough. The maximum current density is 90.6 mA cm^{-2}, about 10 times of that without the presence of Cl^- ions.

Fig. 3 shows the polarization and power curves of an Ni–O_2 fuel cell with a nickel foam anode and an aqueous electrolyte (pH = 11.30–11.50, adjusted by NaOH) of 0.50 mol L^{-1} Na_2SO_4, 2.0 mol L^{-1} $NH_3 \cdot H_2O$, and 0.60 mol L^{-1} NaCl. It is easily seen that the maximum specific power of 15 mW cm^{-2} is generated at the voltage of 0.3 V and current density of 50 mA cm^{-2}. The fuel cell operates stably as shown in Fig. S2, beneficial to the synthesis of $Ni(OH)_2$ with high quality. Because the fuel cell is designed for material synthesis, a large current needs to be chosen instead of a large power. We chose a current of 80% maxima (40 mA cm^{-2}) for synthesizing $Ni(OH)_2$, equivalent to an $Ni(OH)_2$ production rate of 68.6 mg h^{-1} cm^{-2}.

Fig. 4a shows the XRD patterns of the synthesized $Ni(OH)_2$ sample. The XRD peaks located at 2-theta degrees of 19.42°, 33.24°, 38.70°, 52.27° and 59.30°, are corresponding to the reflections of the β-$Ni(OH)_2$ crystalline plans of (001), (100), (101), (102) and (110) (standard XRD pattern: JCPDS #14-0117), respectively. The sample exhibits rather uniformly spherical (ca. 10 μm in diameter) as shown by the low magnification FE-SEM image in Fig. 4b. The spherical particles have flower structure at micrometer scale with thin nano-plates crossed and stacked, as shown by the high magnification FE-SEM image in Fig. 4c. The loose channels between the nano-plates help the migration of protons and electrons, thus enhancing the electrochemical performances of the $Ni(OH)_2$.[19]

The electrochemical performances of the synthesized nano/micro-structured β-$Ni(OH)_2$ sample were investigated by the charge/discharge and cyclic voltammetry (CV) experiments. The charge/discharge experiments were carried out at very high current densities of 1000, 2000, and 5000 mA g^{-1}. After activation period, the charge/discharge curves at 10^{th} cycle in Fig. 4d

show that the discharge capacities of the β-$Ni(OH)_2$ electrode are higher than 260 mAh g^{-1} at current densities of 1000, 2000, and 5000 mA g^{-1}, which are comparable to the capacities of the state-of-the-art β-$Ni(OH)_2$ samples prepared by conventional methods.[15, 19] After 350 cycles, the discharge specific capacities reduce by 7.6%, 8.3%, and 9.2%, respectively, at current densities of 1000, 2000, and 5000 mA g^{-1} as shown in Fig. S3a. As for these high current densities, the results mean that the synthesized β-$Ni(OH)_2$ samples have excellent cycling stability.[15, 19] Besides, the CV curves of the synthesized β-$Ni(OH)_2$ samples in Fig. S3b show an about 300 mV difference between the positions of oxidation peaks and reduction peaks. This indicates an excellent reversibility of the synthesized β-$Ni(OH)_2$ samples.[15, 19]

Conclusions

This study demonstrates the feasibility of an 100% atom-economical route for the synthesis of $Ni(OH)_2$ from nickel metal, water, and O_2 based on a newly designed membrane-free Ni–O_2 fuel cell. The synthesized $Ni(OH)_2$ has the desired nano/micro structure for the positive electrode material and exhibits excellent performance in NiMH batteries. The activation of Ni anode by the complexation of $NH_3 \cdot H_2O$ and Ni^{2+} as well as the destruction of the protecting oxide film by Cl^- ions is the key to the success. This green synthesis is potentially applicable for the syntheses of other metal hydroxides using a metal–O_2 fuel cell. The metal should have a lower standard electrode potential than that of oxygen gas and a protective oxide film on the surface so that it can be stable in water. Appropriate additives thus need to be figured out to active the metal for anodic dissolution.

Experimental

The chemicals of sodium sulfate (Na_2SO_4, 99.5%), sodium chloride (NaCl, 99.5%), aqua ammonia ($NH_3 \cdot H_2O$, 25%), sodium hydroxide (NaOH, 99%) and hydrochloric acid (HCl, 37%) were all analytical reagent grade, which were purchased from Beijing Chemical Factory in China and used as received.

Activation of Ni anode. The study of the activation of Ni anode was carried out in an electrochemical cell with a three-electrode configuration. An Ni foam (300 g m^{-2} in area density, 1 mm in thickness, and 99.5% in purity, Heze Tianyu Technology Company), an Ni wire (99.9% in purity, Beijing Zhongjin Yan new Material Technology Co., Ltd), and an Hg/HgO electrode were, respectively, used as the working electrode, the counter electrode, and the reference electrode. The Ni working electrode was pretreated by rinse with acetone to remove the grease, immersion into a 3.0 mol L^{-1} HCl solution for 10 min to eliminate the passivation film, an oxide film, on the surface, and rinse again with deionized water. To characterize the activation of Ni anodes under different conditions of temperature, concentrations of ammonia and halogen ions, the potentiodynamic polarization experiments were performed at a scanning rate of 2.0 mV s^{-1} between −0.30 V and 0.60 V on a CSU-300 electrochemical workstation (Wuhan Corrtest Instrument). In all of these electrochemical experiments, 0.50 mol L^{-1} Na_2SO_4 was used as the supporting electrolyte.

Ni–O_2 fuel cell and 100% atom-economical synthesis of $Ni(OH)_2$. The Ni–O_2 fuel cell consisted of an Ni foam anode (25 mm × 20 mm), an oxygen cathode made of a carbon paper (25 mm × 20 mm, TGP-H-060, Toray) with a carbon black (Vulcan 72R, Cabot) loading of 0.5 mg cm^{-2} and a catalyst loading of 1.2 mg cm^{-2} (40 wt.% Pt/C, Johnson Matthey), and an aqueous electrolyte containing 0.50 mol L^{-1} Na_2SO_4, 2.0 mol L^{-1} $NH_3 \cdot H_2O$, and 0.60 mol L^{-1} NaCl. The nickel foam anode was pretreated as the study for Ni anode activation. The distance between two

electrodes was 20 mm. The polarization curves and stability curves of the fuel cell were, respectively, recorded potentiostatically and galvanostatically on a battery test station (LAND-CT2001A).

The synthesis of $Ni(OH)_2$ was carried out in a fuel cell (an Ni–O_2 fuel cell) with a nickel foam anode and under the optimized conditions of 55 °C, an aqueous electrolyte (pH = 11.30–11.50, adjusted by NaOH) of 0.50 mol L^{-1} Na_2SO_4, 2.0 mol L^{-1} $NH_3 \cdot H_2O$, and 0.60 mol L^{-1} NaCl. The total amount of electrolyte was 500 mL and circulated between the fuel cell and a sealed tank at a rate of 40 mL min^{-1} using a peristaltic pump during the operation of the fuel cell. The fuel cell operated galvanostatically with a current density of 40 mA cm^{-2}. The synthesized $Ni(OH)_2$ nuclei were carried by the flow of the electrolyte into the tank and stayed there by the block of a glass frit filter with ca. 3 μm nominal pore size. In the tank, the $Ni(OH)_2$ nuclei grow up and form into the nano/micro structure.

Physical characterizations. The powder X-ray diffraction (XRD) patterns of the synthesized $Ni(OH)_2$ were obtained on a Rigaku D/max2500VB2+/PC diffractometer with Cu Kα radiation (λ = 0.15418 nm, 40 kV, 200 mA) at a scanning rate of 10 °/min with a step size of 0.02° (0.12 s/step). A field emission – scanning electron microscope (FE-SEM, Hitachi S4700) was used to characterize the morphology of the Ni anodes and the synthesized $Ni(OH)_2$ samples. The discharged Ni anodes were taken out from the fuel cell and quickly placed in an N_2 filled container to avoid the oxidation by air before FE-SEM characterization.

Electrochemical characterizations of the synthesized $Ni(OH)_2$. The mixture of as-prepared 0.20 g $Ni(OH)_2$ and 0.050 g expanded graphite powders (OER-CX200, China Sciences Hengda Graphite Co., Ltd) was ground with an agate pestle and mortar. The mixture was further ground with an amount of 5 wt.% polytetrafluoroethylene (PTFE) suspension (60 wt.%,

Guangzhou Songbai Chemicals Company) and then fed into a roller press to fabricate a film 80 μm in thick. This film was pressed on a piece of Ni foam to obtain the working electrode. A three-electrode configuration was built with this working electrode, a Zn/ZnO electrode (home-made) as the reference electrode,[19] and a Ni wire as the counter electrode. The three electrodes sit still in an aqueous electrolyte (6.0 mol L^{-1} KOH) for 3 h for equilibrium. The charging/discharging experiments and cyclic voltammetry experiments were, respectively, carried out on a battery test station (LAND-CT2001A) and a CSU-300 electrochemical workstation (Wuhan Corrtest Instrument).[19] The discharge specific capacity was calculated based on the mass of nickel hydroxide in the electrode.

Acknowledgments: The work at Beijing University of Chemical Technology (BUCT, China) was supported by the State Key Program of National Natural Science of China (No. 21236003), National Natural Science Foundation of China (No. 21476022) and Beijing Higher Education Young Elite Teacher Project (YETP0509).

References:

1. P. Bocchetta, M. Santamaria and F. Di Quarto, *Electrochem. Commun.*, 2007, **9**, 683-688.
2. F. Y. Cheng, J. Chen, X. L. Gou and P. W. Shen, *Adv. Mater.*, 2005, **17**, 2753-2756.
3. S. Zhu, H. Zhou, T. Miyoshi, M. Hibino, I. Honma and M. Ichihara, *Adv. Mater.*, 2004, **16**, 2012-2017.
4. Y. Sun, X. Hu, W. Luo and Y. Huang, *ACS Nano*, 2011, **5**, 7100-7107.
5. Y. Gu, D. Chen and X. Jiao, *J. Phys. Chem. B*, 2005, **109**, 17901-17906.
6. M. Geng and D. O. Northwood, *Int. J. Hydrogen Energy*, 2003, **28**, 633-636.
7. M. Casas-Cabanas, J. Canales-Vázquez, J. Rodríguez-Carvajal and M. R. Palacín, *J. Am. Chem. Soc.*, 2007, **129**, 5840-5842.
8. D. M. MacArthur, *J. Electrochem. Soc.*, 1970, **117**, 422-426.

9. Y.-K. Sun, S.-T. Myung, M.-H. Kim, J. Prakash and K. Amine, *J. Am. Chem. Soc.*, 2005, **127**, 13411-13418.
10. W. Luo, X. Li and J. R. Dahn, *Chem. Mater.*, 2010, **22**, 5065-5073.
11. K. M. Shaju and P. G. Bruce, *Adv. Mater.*, 2006, **18**, 2330-2334.
12. K. C. Ho and J. Jorné, *J. Electrochem. Soc.*, 1990, **137**, 149-158.
13. M. J. Avena, M. V. Vazquez, R. E. Carbonio, C. P. Pauli and V. A. Macagno, *J. Appl. Electrochem.*, 1994, **24**, 256-260.
14. M. Akinc, N. Jongen, J. Lemaître and H. Hofmann, *J. Eur. Ceram. Soc.*, 1998, **18**, 1559-1564.
15. F.-S. Cai, G.-Y. Zhang, J. Chen, X.-L. Gou, H.-K. Liu and S.-X. Dou, *Angew. Chem. Int. Ed.*, 2004, **43**, 4212-4216.
16. Y. Li, W. Li, S. Chou and J. Chen, *J. Alloys Compd.*, 2008, **456**, 339-343.
17. P. Jeevanandam, Y. Koltypin and A. Gedanken, *Nano Lett.*, 2001, **1**, 263-266.
18. M. Vidotti, C. van Greco, E. A. Ponzio and S. I. Córdoba de Torresi, *Electrochem. Commun.*, 2006, **8**, 554-560.
19. X. Yue, J. Pan, Y. Sun and Z. Wang, *Ind. Eng. Chem. Res.*, 2012, **51**, 8358-8365.
20. Univertical Corporation, http://www.univertical.cn/en/products03.htm, (accessed Oct. 2014).
21. B. Trost, *Science*, 1991, **254**, 1471-1477.
22. B. R. Reddy, C. Parija and P. V. R. B. Sarma, *Hydrometallurgy*, 1999, **53**, 11-17.
23. J. L. Trompette, L. Massot and H. Vergnes, *Corros. Sci.*, 2013, **74**, 187-193.
24. Y. Li, X. Fan, N. Tang, H. Bian, Y. Hou, Y. Koizumi and A. Chiba, *Corros. Sci.*, 2014, **78**, 101-110.
25. W. Li, T. Cochell and A. Manthiram, *Sci. Rep.*, 2013, **3,** 1229:1-7
26. N. Hackerman, E. S. Snavely Jr and L. D. Fiel, *Electrochim. Acta*, 1967, **12**, 535-551.
27. B. Löchel, H. H. Strehblow and M. Sakashita, *J. Electrochem. Soc.*, 1984, **131**, 522-529.
28. B. P. Löchel and H. H. Strehblow, *J. Electrochem. Soc.*, 1984, **131**, 713-723.

Competing financial interests: The authors declare no competing financial interests.

Schematic and Figure legends

Schematic 1 Flowcharts for the preparation of ($Ni(OH)_2$) by (a) a conventional process and (b) a nickel–oxygen ($Ni–O_2$) fuel cell. The calculation for atom economy is in the supplementary information.

Fig. 1 Diagram of the $Ni–O_2$ fuel cell. The diffusion layer is a carbon paper (TGP-H-060, Toray) coated with carbon black (Vulcan 72R, Cabot). The cathode catalyst is platinum nanoparticles supported on carbon black (40 wt.% Pt/C, JM40, Johnson Matthey).

Fig. 2 Anode polarization curves with (a) different concentrations of $NH_3 \cdot H_2O$ and 0.50 mol L^{-1} Na_2SO_4, and (b) different halogen ions (0.5 mol L^{-1}), 0.50 mol L^{-1} Na_2SO_4, and 2.0 mol L^{-1} $NH_3 \cdot H_2O$; FE-SEM images of the Ni foam anode (c) before and (d) after reaction; and (e) anode polarization curves with different concentrations of Cl^- ions, 0.50 mol L^{-1} Na_2SO_4, and 2.0 mol L^{-1} $NH_3 \cdot H_2O$. All of the electrolytes had a pH range of 11.30–11.50. The potential scanning rates were 2 mV s^{-1} and the temperature was 55 °C.

Fig. 3 Polarization and power curves of the $Ni–O_2$ fuel cell. The fuel cell operated with a nickel foam anode and an aqueous electrolyte (pH = 11.30–11.50, adjusted by NaOH) of 0.50 mol L^{-1} Na_2SO_4, 2.0 mol L^{-1} $NH_3 \cdot H_2O$, and 0.60 mol L^{-1} NaCl at 55 °C.

Fig. 4 (a) X-ray diffraction pattern, (b) low magnification and (c) high magnification field emission – scanning electron microscope (FE-SEM) images of the nano/micro structured β-$Ni(OH)_2$ sample synthesized in an $Ni–O_2$ fuel cell at 40 mA cm^{-2} at 55 °C, (d) its

charge/discharge curves in three-electrode configuration electrochemical cell. The fuel cell employed a nickel foam anode and an aqueous electrolyte (pH = 11.30–11.50, adjusted by NaOH) of 0.50 mol L^{-1} Na_2SO_4, 2.0 mol L^{-1} $NH_3 \cdot H_2O$, and 0.60 mol L^{-1} NaCl.

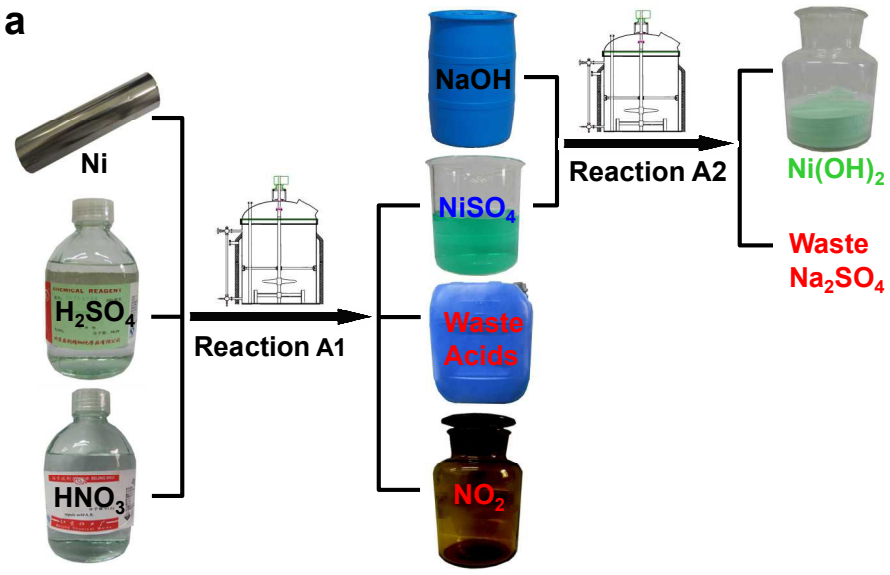

A1: $Ni+H_2SO_4+2HNO_3 = NiSO_4+2NO_2+2H_2O$ atom economy = 54.7%

A2: $NiSO_4+2NaOH = Ni(OH)_2+Na_2SO_4$ atom economy = 39.5%

The atom economy of the route = 54.7% x 39.5% = 21.6%

Raw Materials (RM); Intermediate; Waste; Target Product (TP)

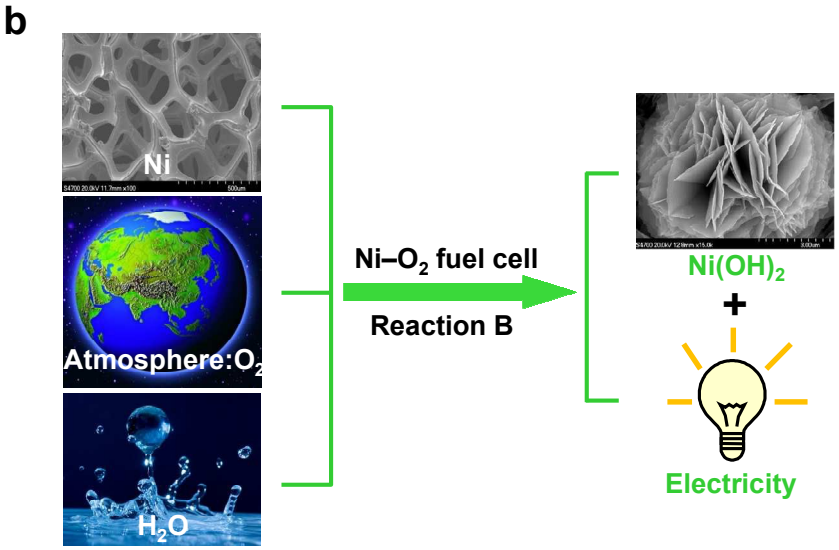

B: $Ni + 1/2O_2 + H_2O = Ni(OH)_2$ atom economy = 100%

The atom economy of the route = 100%

Raw Materials (RM); Target Product (TP)

Schematic 1 Flowcharts for the preparation of ($Ni(OH)_2$) by (a) a conventional process and (b) a nickel–oxygen ($Ni–O_2$) fuel cell. The calculation for atom economy is in the supplementary

information.

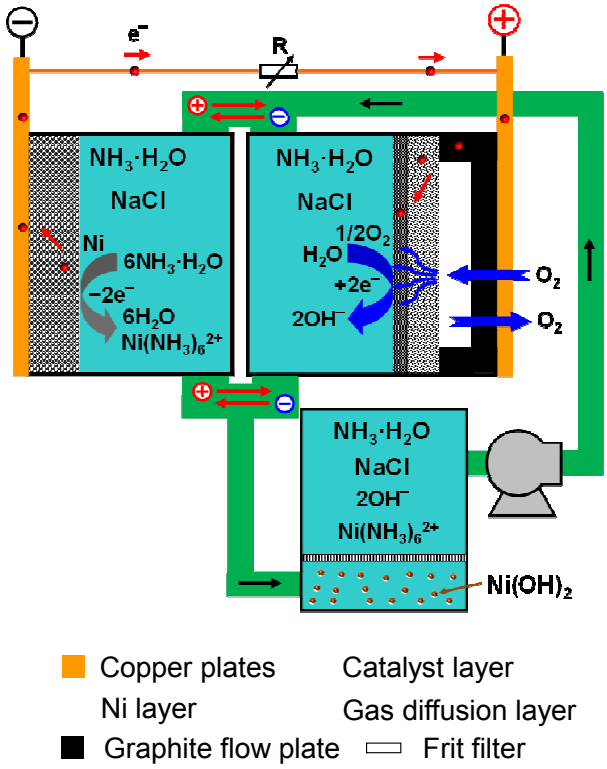

Fig. 1 Diagram of the Ni–O_2 fuel cell. The diffusion layer is a carbon paper (TGP-H-060, Toray) coated with carbon black (Vulcan 72R, Cabot). The cathode catalyst is platinum nanoparticles supported on carbon black (40 wt.% Pt/C, JM40, Johnson Matthey).

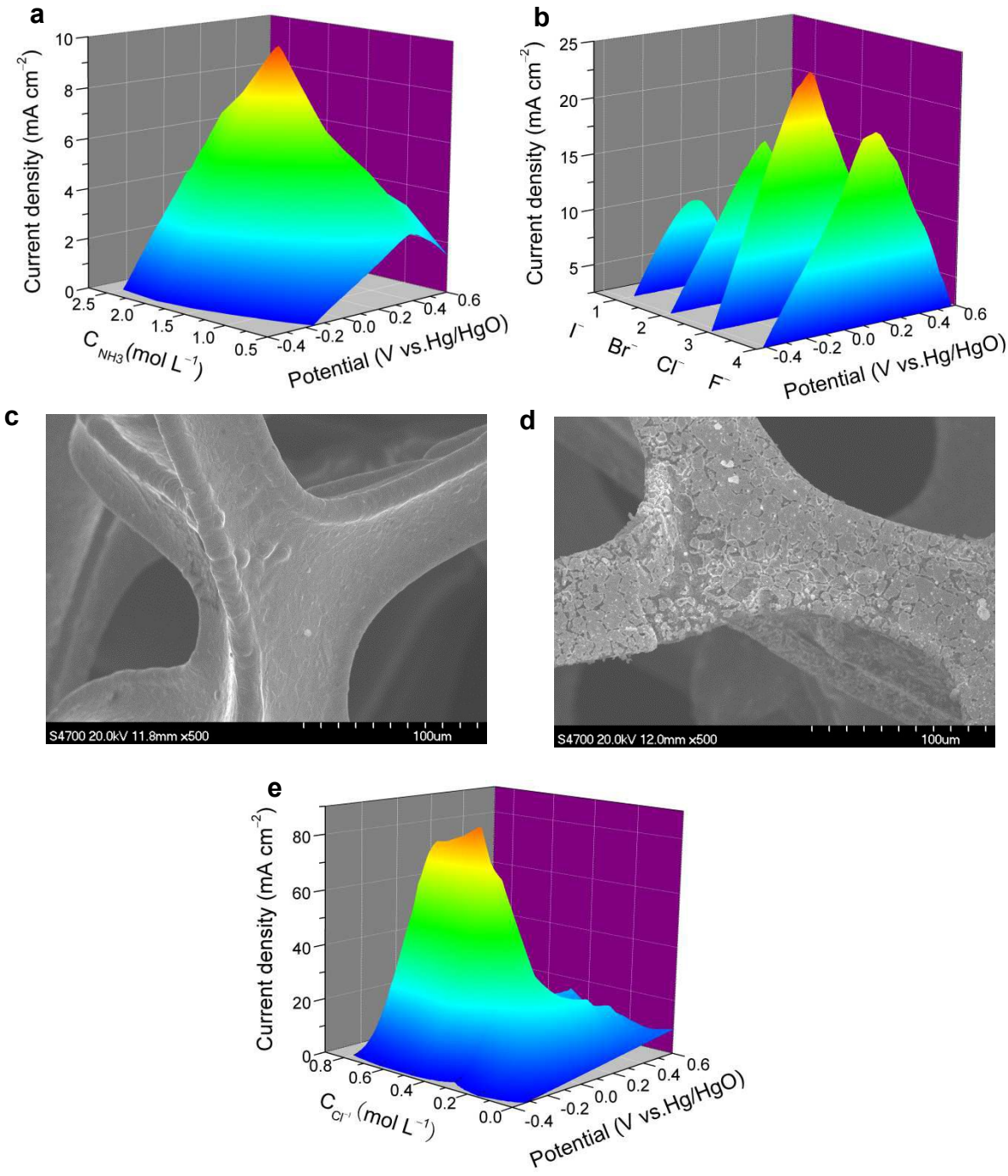

Fig. 2 Anode polarization curves with (a) different concentrations of $NH_3 \cdot H_2O$ and 0.50 mol L^{-1} Na_2SO_4, and (b) different halogen ions (0.5 mol L^{-1}), 0.50 mol L^{-1} Na_2SO_4, and 2.0 mol L^{-1} $NH_3 \cdot H_2O$; FE-SEM images of the Ni foam anode (c) before and (d) after reaction; and (e) anode polarization curves with different concentrations of Cl^- ions, 0.50 mol L^{-1} Na_2SO_4, and 2.0 mol

L^{-1} $NH_3 \cdot H_2O$. All of the electrolytes had a pH range of 11.30–11.50. The potential scanning rates were 2 mV s^{-1} and the temperature was 55 °C.

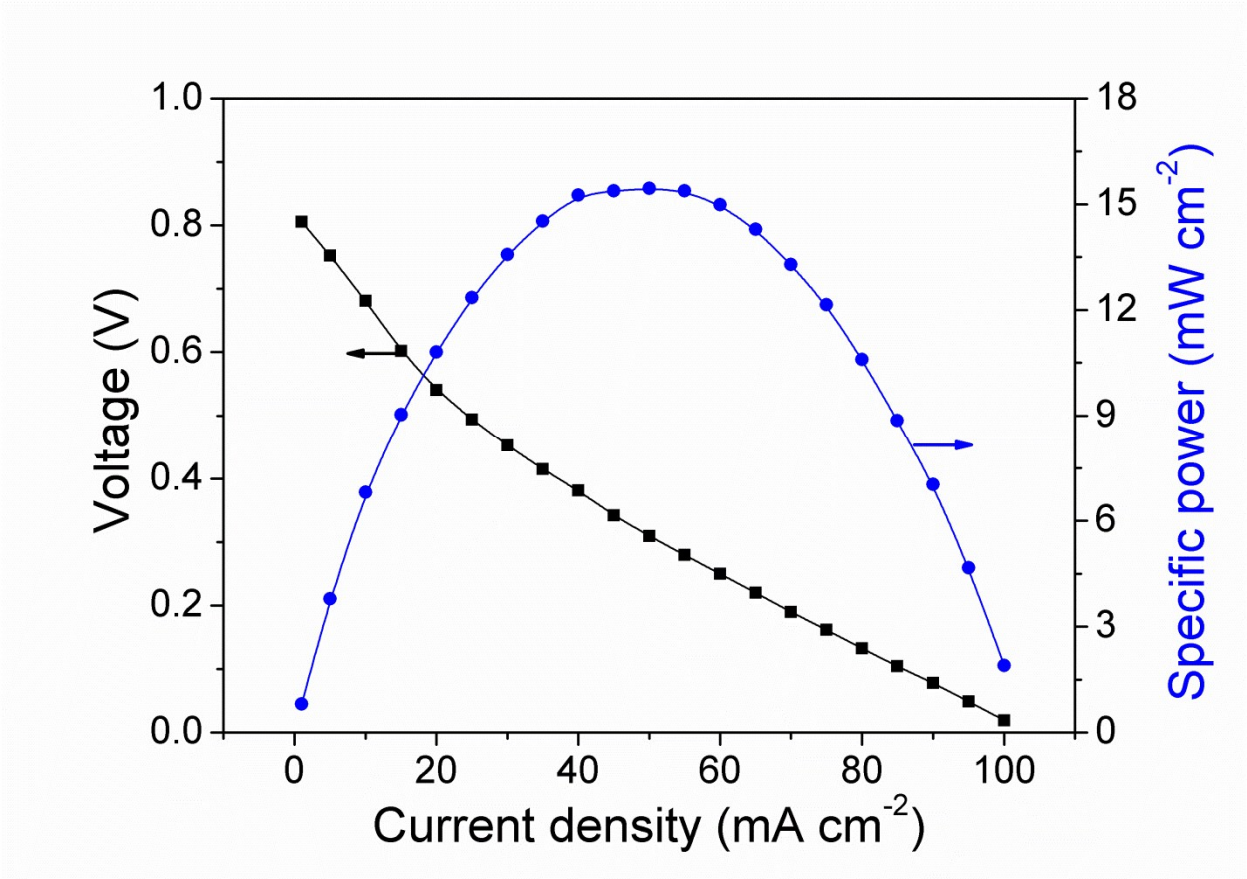

Fig. 3 Polarization and power curves of the Ni–O_2 fuel cell. The fuel cell operated with a nickel foam anode and an aqueous electrolyte (pH = 11.30–11.50, adjusted by NaOH) of 0.50 mol L^{-1} Na_2SO_4, 2.0 mol L^{-1} $NH_3 \cdot H_2O$, and 0.60 mol L^{-1} NaCl at 55 °C.

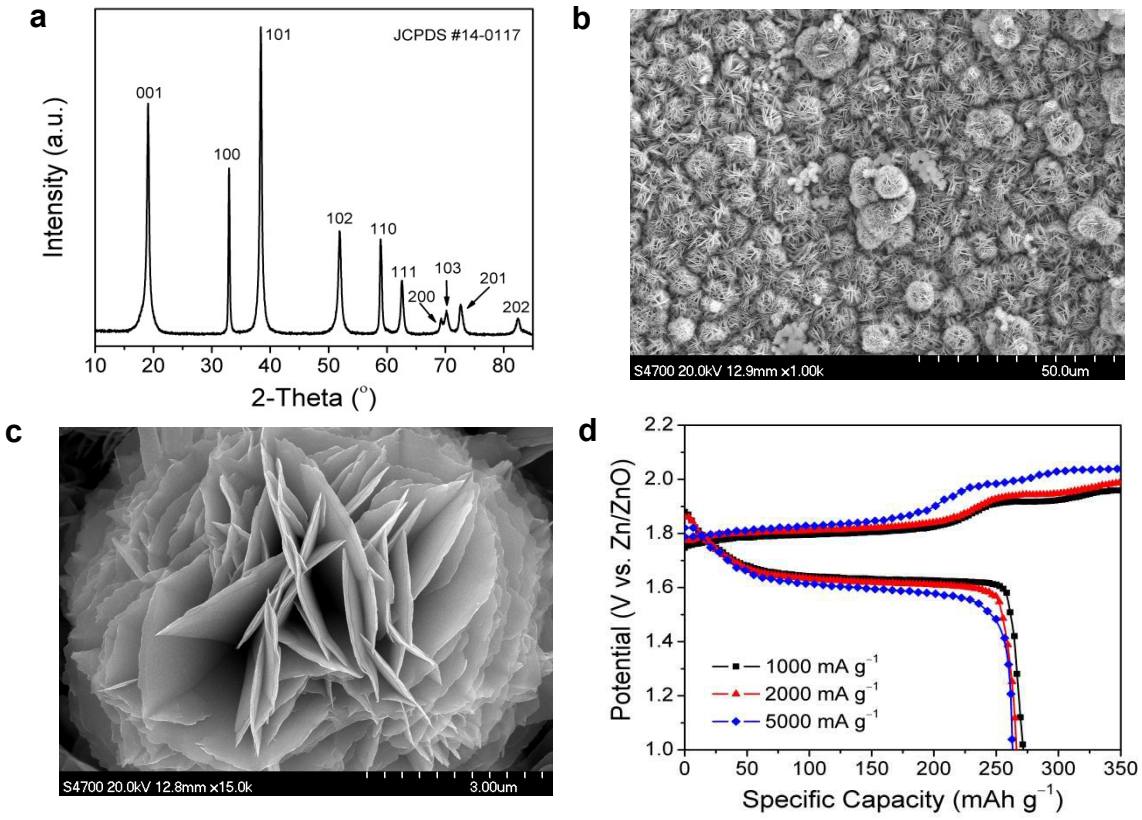

Fig. 4 (a) X-ray diffraction pattern, (b) low magnification and (c) high magnification field emission – scanning electron microscope (FE-SEM) images of the nano/micro structured β-$Ni(OH)_2$ sample synthesized in an Ni–O_2 fuel cell at 40 mA cm^{-2} at 55 °C, (d) its charge/discharge curves in three-electrode configuration electrochemical cell. The fuel cell employed a nickel foam anode and an aqueous electrolyte (pH = 11.30–11.50, adjusted by NaOH) of 0.50 mol L^{-1} Na_2SO_4, 2.0 mol L^{-1} $NH_3 \cdot H_2O$, and 0.60 mol L^{-1} NaCl.